Annals of Nuclear Medicine Vol. 14, No. 5, 323–328, 2000

Evaluation of ^{62}Cu labeled diacetyl-bis(N^4-methylthiosemicarbazone) as a hypoxic tissue tracer in patients with lung cancer

Norio TAKAHASHI,* Yasuhisa FUJIBAYASHI,** Yoshiharu YONEKURA,**
Michael J. WELCH,*** Atsuo WAKI,** Tatsuro TSUCHIDA,*
Norihiro SADATO,** Katsuya SUGIMOTO* and Harumi ITOH*

*Department of Radiology and **Biomedical Imaging Research Center, Fukui Medical University, Fukui, Japan
***Mallinckrodt Institute of Radiology, Washington University School of Medicine, St. Louis, MO, USA

^{62}Cu labeled diacetyl-bis(N^4-methylthiosemicarbazone) (^{62}Cu-ATSM) has been proposed as a generator-produced, positron-emitting tracer for hypoxic tissue imaging. From basic studies, the retention mechanism of ^{62}Cu-ATSM is considered to be closely related to cytosolic/microsomal bioreduction, a possible system for hypoxic bioreductive drug activation. In order to evaluate the characteristics of ^{62}Cu-ATSM, PET studies were performed in 4 normal subjects and 6 patients with lung cancer. ^{62}Cu-ATSM cleared rapidly from the blood with little lung uptake (0.43 ± 0.09, uptake ratio; divided by the arterial input function) in normal subjects. Intense tumor uptake of ^{62}Cu-ATSM was observed in all patients with lung cancer (3.00 ± 1.50). A negative correlation was observed between blood flow and flow-normalized ^{62}Cu-ATSM uptake in three of four patients. In contrast, ^{62}Cu-ATSM uptake was not related to that of ^{18}F-fluorodeoxyglucose. The negative correlation between blood flow and flow normalized ^{62}Cu-ATSM uptake suggests an enhancement of retention of ^{62}Cu-ATSM by low flow. ^{62}Cu-ATSM is a promising PET tracer for tumor imaging, which might bring new information for chemotherapeutic treatment as well as radiotherapy of hypoxic tumors.

Key words: ^{62}Cu-ATSM, hypoxia, lung cancer, ^{18}F-FDG, PET

INTRODUCTION

HYPOXIA in tumors may be an important factor in resistance to radiotherapy as well as chemotherapy.[1,2] Nitroimidazole compounds are of great interest because they are reduced enzymatically and trapped in regions of low oxygen tension.[3] Based on these considerations, various groups have attempted to design nitroimidazole-based drugs labeled with ^{18}F,[4] ^{123}I,[5] or ^{99m}Tc[6] for imaging hypoxia, but these drugs had low target accumulation due to slow blood clearance and low membrane permeability.[7]

^{62}Cu labeled diacetyl-bis(N^4-methylthiosemicarbazone) (^{62}Cu-ATSM) has been proposed as a generator-produced, positron-emitting tracer for imaging hypoxia.[8] ^{62}Cu-PTSM, developed as a perfusion tracer, is easily reduced by the electron transport system of mitochondria, which explains its retention.[9] On the other hand, ^{62}Cu-ATSM, an analogue of ^{62}Cu-PTSM, cannot be reduced by normal mitochondria due to its low redox potential. As a result, although it has high membrane permeability, it is not retained in normal brain and heart tissue, but accumulates in hypoxic tissue where it is more easily reduced.[10] Therefore, ^{62}Cu-ATSM is a better candidate for a hypoxia imaging agent than nitroimidazole-based drugs because of its higher membrane permeability. It has been reported that ^{64}Cu-ATSM has been selectively trapped *in vitro* in EMT6 cells under hypoxic conditions and *in vivo* in solid EMT6 tumors.[11] To evaluate the characteristics of ^{62}Cu-ATSM in humans, PET studies were performed on 4 normal subjects and 6 patients with lung cancer.

Received March 2, 2000, revision accepted May 26, 2000.
For reprint contact: Tatsuro Tsuchida, M.D., Department of Radiology, Fukui Medical University, Shimoaizuki, Matsuoka-cho, Yoshida-gun, Fukui 910–1137, JAPAN.
E-mail: tsucchy@fmsrsa.fukui-med.ac.jp

Table 1 Summary of clinical and imaging data of patients with lung cancer

Patient no.	Age (yr)	Sex	Pathological diagnosis	Size (cm)	Blood flow (ml/min/100 g)	FDG SUV (mg/ml)	^{62}Cu-ATSM Uptake ratio
1.	72	M	Squamous cell carcinoma	8.0	na	6.92 ± 4.08	2.04 ± 1.17
2.	67	F	Adenocarcinoma	3.8	11.67 ± 5.86	8.18 ± 1.18	1.18 ± 0.40
3.	84	M	Squamous cell carcinoma	5.6	na	9.00 ± 2.66	5.24 ± 3.10
4.	49	F	Metastasis (breast cancer)	5.0	15.39 ± 4.83	7.76 ± 2.13	2.35 ± 0.81
5.	87	M	Squamous cell carcinoma	4.2	3.51 ± 2.18	8.51 ± 3.56	2.00 ± 0.34
6.	73	M	Adenocarcinoma	11.0	3.94 ± 2.73	5.55 ± 2.26	4.56 ± 2.39

Blood flow, SUV and Uptake ratio are mean ± S.D., na = not available

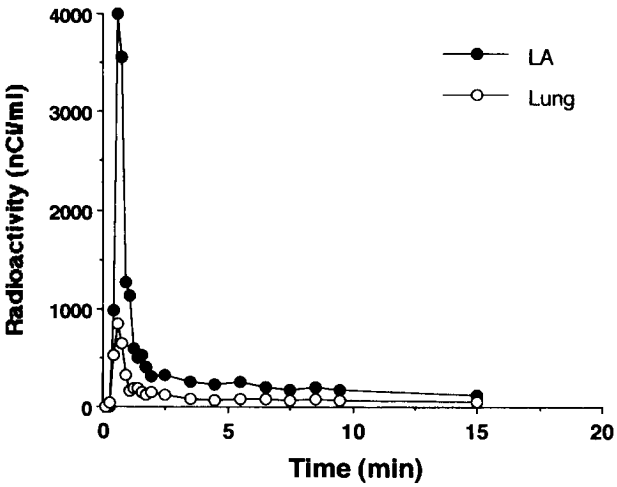

Fig. 1 Representative time activity curves of the left atrium (LA) and lung obtained from serial dynamic PET scan after ^{62}Cu-ATSM injection to a normal volunteer.

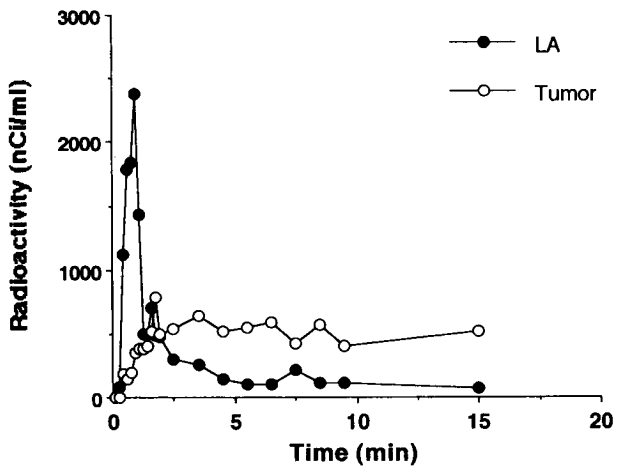

Fig. 2 Representative time activity curves of the left atrium (LA) and lung cancer (patient no. 6) obtained from serial dynamic PET scan after ^{62}Cu-ATSM injection.

MATERIALS AND METHODS

Preparation of ^{62}Cu-ATSM

^{62}Cu was obtained with a ^{62}Zn/^{62}Cu generator system from [^{62}Zn]$ZnCl_2$ solution.[12] Cu-ATSM was synthesized according to the method of Gingas et al.,[13] and confirmed by elemental analysis and mass spectrometry. ^{62}Cu-ATSM was prepared as follows[8]: Briefly, four ml of ^{62}Cu-glycine (non-carrier added ^{62}Cu) solution obtained from the generator was mixed with 0.2 ml of ATSM solution (0.4 mM in dimethyl sulfoxide). The radiochemical purity of ^{62}Cu-ATSM was confirmed with HPLC in combination with authentic Cu-ATSM.

Subjects

The study involved 4 normal male volunteers (ages 34–64 yrs) and 6 patients with lung cancer (4 males and 2 females, ages 49–87 yrs). Altogether there were 2 adenocarcinomas, 3 squamous cell carcinomas and 1 metastasis from breast cancer (Table 1). All the patients were investigated with both ^{62}Cu-ATSM and ^{18}F-fluorodeoxyglucose. Four of the 6 patients were also evaluated by ^{15}O-water. The study was approved by the Ethical Committee of Fukui Medical University and written informed consent was obtained from all the subjects before the PET study.

PET

PET was performed with a high-resolution, whole-body PET scanner with an 18-ring detector arrangement (Advance, GE Medical Systems, Milwaukee). The physical characteristics of this scanner have been described in detail by DeGrado et al.[14] Briefly, the system permits the simultaneous acquisition of 35 transaxial images with an interslice spacing of 4.25 mm. Both axial and transaxial resolution are 4.2 mm, allowing multidirectional reconstruction of the images without loss of resolution. The FOV and the pixel size of the reconstructed images were 256 and 2 mm, respectively. A 10-min transmission scan was acquired with a ^{68}Ge/^{68}Ga source for attenuation correction, followed by intravenous injection of 370 to 740 MBq of ^{62}Cu-ATSM over 30 sec. PET data acquisition was started at the time of ^{62}Cu-ATSM injection and continued for 20 minutes in 10-sec frames for the first 120 sec, 60-sec frames for the next 8 min and a final 10-min frame. In order to evaluate the side effects of ^{62}Cu-ATSM, physical examinations and hematological and biochemical data analysis were performed before and after administration of ^{62}Cu-ATSM.

To compare ^{62}Cu-ATSM images with blood flow and

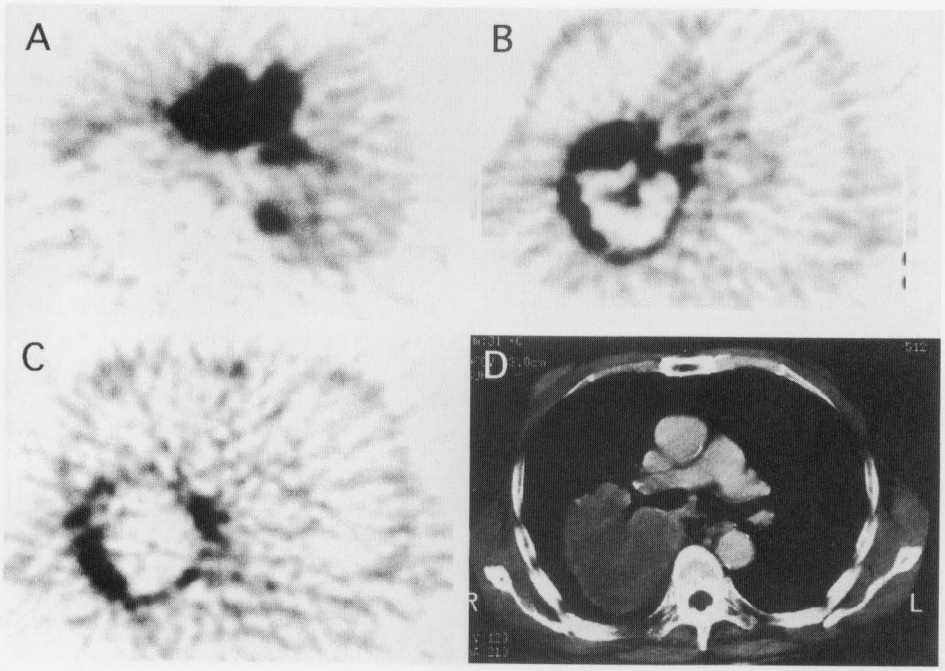

Fig. 3 A 73-yr-old man with adenocarcinoma in the right lower lobe (patient no. 6). The blood flow (A), FDG (B), ^{62}Cu-ATSM (C) and contrast-enhanced CT (D) images are shown.

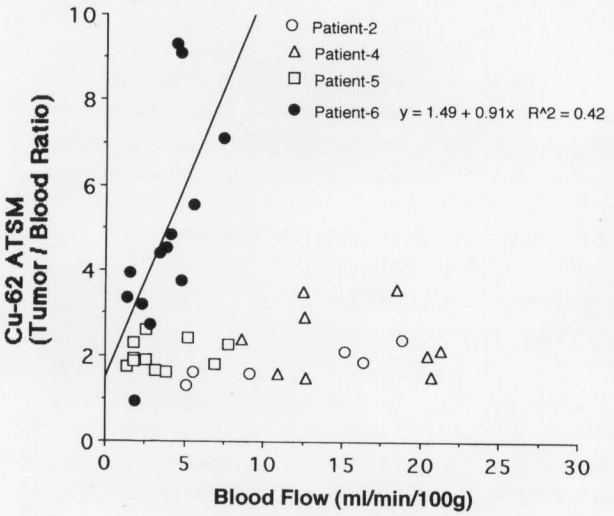

Fig. 4 The blood flow was plotted against its ^{62}Cu-ATSM uptake ratio for tumor segments in each patient with lung cancer. The least square linear regression line and equation are also shown.

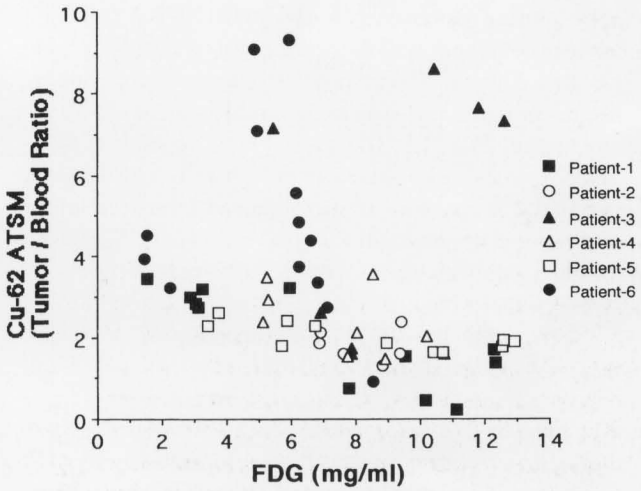

Fig. 5 The FDG uptake (SUV) was plotted against its ^{62}Cu-ATSM uptake ratio for tumor segments in each patient with lung cancer.

glucose metabolism of tumors, ^{15}O-water and FDG PET was performed within one week. After approximately 1110 MBq of ^{15}O-water was injected intravenously, a serial dynamic PET scan was performed for 120 sec in 4 of 6 patients. In all 6 patients, approximately 370 MBq of FDG was injected intravenously after a 4-hr fast. A static scan was performed for 20 min (40–60 min postinjection).

Data Analysis

In the normal volunteer study, circular regions of interest (ROIs) were placed on the dynamic ^{62}Cu-ATSM PET images of the lung and left atrium (22.9 cm^2 and 1.8 cm^2 respectively in area). The last frame, which was obtained 10–20 min after the injection, was used as a static image and the lung activity of ^{62}Cu-ATSM was normalized by the arterial blood activity, which was derived from the ROI placed over the left atrium of the PET image (uptake

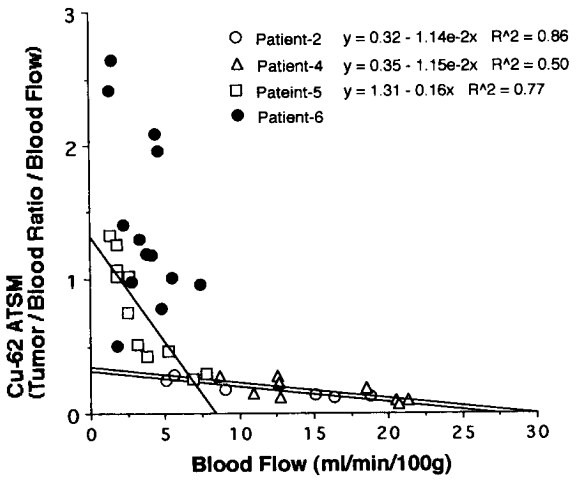

Fig. 6 The blood flow was plotted against its normalized ^{62}Cu-ATSM uptake ratio for tumor segments in each patient with lung cancer. The least square linear regression line and equation are also shown.

ratio). The other circular ROIs were placed on the static image of the left myocardium and liver (0.6 cm^2 and 22.9 cm^2 respectively in area) and the uptake ratio of those organs was obtained.

In patients with lung cancer, multiple circular ROIs (> 0.6 cm^2 in area) were placed over the ^{62}Cu-ATSM PET images of tumors, and the uptake ratio was calculated as described above. The blood flow images were calculated from ^{15}O-water PET data in each subject by an autoradiographic method.[15–17] The arterial input function was derived from the radioactivity in the left atrium by using the circular 1.8 cm^2-ROI in area, instead of arterial blood sampling. The standardized uptake value (SUV) images of FDG were calculated with the following formula:

$$\text{SUV} = \text{radioactivity concentration (Bq/m}l\text{)} / \{\text{injected dose (Bq)} / \text{body weight (g)}\}$$

The same ROIs as used in the ^{62}Cu-ATSM PET images of tumors were placed on both the blood flow and SUV images, and the uptake ratio of ^{62}Cu-ATSM was compared with the blood flow and SUV of FDG in each patient. In addition, the uptake ratio was normalized by its absolute blood flow value. The flow-normalized uptake ratio was compared with the blood flow.

RESULTS

^{62}Cu-ATSM rapidly cleared from the blood, reaching a stable activity level a few minutes after the injection (Fig. 1). Little uptake was observed in the lung (uptake ratio: 0.43 ± 0.09). The left myocardial uptake was small (1.84 ± 0.35), but the liver uptake was considerable (2.45 ± 1.03). No side effects were observed in any of the four subjects.

^{62}Cu-ATSM rapidly accumulates in tumors, reaching plateau levels within a few minutes after the injection (Fig. 2). An abnormally intense uptake of ^{62}Cu-ATSM was observed in all patients with lung cancer (uptake ratio: 3.00 ± 1.50), but the distribution pattern of ^{62}Cu-ATSM is different from that of FDG or blood flow (Fig. 3). No correlation was observed between ^{62}Cu-ATSM and the blood flow pattern except in one patient (Fig. 4). No correlation between ^{62}Cu-ATSM and FDG was found (Fig. 5). In three of four patients, a negative correlation was observed between blood flow and the flow-normalized ^{62}Cu-ATSM uptake ratio (Fig. 6).

DISCUSSION

^{62}Cu-ATSM was rapidly cleared from the blood with little lung uptake in normal subjects. As normal myocardial uptake was small, ^{62}Cu-ATSM also can be used for the evaluation of myocardial hypoxia in patients with ischemic heart disease. The intense liver uptake was expected because it was reported that ^{62}Cu-ATSM was cleared through the liver and kidneys and the liver uptake was the highest among the all organs in mice after 5 min.[11]

Intense tumor uptake of ^{62}Cu-ATSM was observed in all six patients with lung cancer. The ^{62}Cu-ATSM uptake did not correlate with that of FDG. This finding suggests that ^{62}Cu-ATSM uptake may represent characteristics of tumors independent of those represented by FDG uptake. A negative correlation between blood flow and flow-normalized ^{62}Cu-ATSM uptake suggests increased retention of ^{62}Cu-ATSM in low flow areas, but other factors may affect the tumor retention of ^{62}Cu-ATSM since the slope of the correlation differed among subjects. From the results of *in vitro* studies of our group with cultured tumor cells, a reduction in ^{62}Cu-ATSM was shown to be closely related to cytosolic/microsomal bioreduction and was enhanced by hypoxia.[18] This is a possible system for hypoxic, bioreductive drug activation. Higher tumor uptake of ^{62}Cu-ATSM may reflect a higher sensitivity to bioreductive drugs than that to irradiation, because the reduction in ^{62}Cu-ATSM is closely related to bioreductive drug activation, which is enhanced by hypoxic conditions.[18] Accordingly, it may be possible to determine more effective therapies with ^{62}Cu-ATSM PET before treatment.

Although we have not compared ^{62}Cu-ATSM and ^{18}F-fluoromisonidazole (^{18}F-FMISO) in this study, ^{62}Cu-ATSM has three advantages. First, ^{62}Cu can be obtained by a generator system from ^{62}Zn, which has a 9 hr half-life and could be delivered long distance. The second advantage is that the faster tumor uptake of ^{62}Cu-ATSM than of ^{18}F-FMISO allows more rapid imaging of tumors. In ^{18}F-FMISO PET, the difference between normal and hypoxic tissues does not become clear until 2 hours post injection due to slow blood clearance and the low tumor to soft tissue ratio.[7] ^{62}Cu-ATSM PET imaging can be done

within 20 min after injection due to its high membrane permeability,[10] so that the more efficient uptake and washout kinetics of ^{62}Cu-ATSM in lung tumors in comparison with ^{18}F-FMISO offers the possibility of a faster and more efficient means of evaluating of tumor hypoxia by PET imaging. The third advantage is that the uptake of ^{62}Cu-ATSM may be higher than that of ^{18}F-FMISO. The mean tumor uptake ratio of ^{62}Cu-ATSM was 3.00 and maximum uptake was 9.33. In contrast, the maximum tumor/plasma ^{18}F-FMISO ratio was reported to be from 0.9 to 1.5 among 3 patients, although one patient's was 2.3.[7] It was reported that with ^{18}F-FMISO, binding to EMT6 cells starts at a higher oxygen concentrations than with ^{64}Cu-ATSM and the percentage uptake of ^{18}F-FMISO is also much lower than that of ^{64}Cu-ATSM after a longer incubation time.[11]

There are some limitations in this study. Hypoxia in the tumor tissue was not confirmed directly in this study, but electrode measurement of intratumoral pO_2 in patients with lung cancer is highly invasive and technically demanding and it is impossible to analyze hypoxia in a number of segments of tumor, because of an increasing risk of pneumothorax. Increased myocardial retention of ^{62}Cu-ATSM under hypoxic conditions also has been reported in perfused rat hearts.[8] It was also proved that hypoxic retention of ^{62}Cu-ATSM is a reversible phenomenon and is dependent only upon pO_2 and not upon irreversible cellular damage such as membrane disruption.[8] In the *in vitro* study with the EMT6 carcinoma cell line, the uptake of ^{64}Cu-ATSM was related in a sigmoidal fashion to the pO_2 of the media where retention was greatly increased under hypoxic and anoxic conditions.[11] Enhanced retention of ^{62}Cu-ATSM by low flow in this study may indicate that the intense uptake of ^{62}Cu-ATSM reflects a hypoxic condition. Another limitation is that the number of patients was small and the results are preliminary, but intense tumor uptake of ^{62}Cu-ATSM was observed in all six patients with lung cancer and imaging was completed only 20 minutes after injection. Higher tumor uptake of ^{62}Cu-ATSM may reflect higher sensitivity to bioreductive drugs than to irradiation, because the retention mechanism of ^{62}Cu-ATSM is closely related to the bioreductive drug activation, which is enhanced by hypoxic conditions.[18] Accordingly, it may be possible to determine a more effective therapy with ^{62}Cu-ATSM PET before treatment. Appropriate clinical trials are necessary to clarify this question.

In conclusion, this preliminary study suggests that ^{62}Cu-ATSM is a promising PET tracer for tumor imaging, which may provide new information on radiotherapy as well as chemotherapy of hypoxic tumors.

ACKNOWLEDGMENT

We thank Nihon Medi-Physics Co. Ltd., Japan, for supplying ^{62}Zn.

REFERENCES

1. Coleman CN. Hypoxia in tumors: A paradigm for the approach to biochemical and physiological heterogeneity. *J Natl Cancer Inst* 80: 310–317, 1998.
2. Teicher BA, Lazo JS, Sartorelli AC. Classification of antineoplastic agents by their selective toxicities toward oxygenated and hypoxic tumor cells. *Cancer Res* 41(1): 73–81, 1981.
3. Chapman JD, Baer K, Lee J. Characteristics of the metabolism-induced binding of misonidazole to hypoxic mammalian cells. *Cancer Res* 43: 1523–1528, 1983.
4. Jerabek PA, Patrick TB, Kilbourn MR, Dischino DD, Welch MJ. Synthesis and biodistribution of ^{18}F-labeled fluoromisonidazoles: potential *in vivo* markers of hypoxic tissue. *Int J Radiate App Instrum [A]* 37: 599–605, 1986.
5. Mannan RH, Somayaji VV, Lee J, Mercer JR, Chapman JD, Wiebe LI. Radiolabeled 1-(5-iodo-5-deoxy-β-D-arabinofuranosyl)-2-nitroimidazole (iodoazomycin arabinoside: IAZA): a novel marker of tissue hypoxia. *J Nucl Med* 32: 1764–1770, 1991.
6. Linder KE, Chan YW, Cyr JE, Malley MF, Nowotnik DP, Nunn AD. Technetium-O(PnAO-(2-nitroimidazole)) [BMS181321], a new technetium-containing nitroimidazole complex for imaging hypoxia: synthesis characterization and xanthine oxidase-catalyzed reduction. *J Med Chem* 37: 9–17, 1994.
7. Koh WJ, Rasey JS, Evans ML, Grierson JR, Lewellen TK, Graham MM, et al. Imaging of hypoxia in human tumors with [F-18]fluoromisonidazole. *Int J Radiate Once Boil Phys* 22: 199–212, 1992.
8. Fujibayashi Y, Taniuchi H, Yonekura Y, Ohtani H, Konishi J, Yokoyama A. Copper-62-ATSM: a new hypoxia imaging agent with high membrane permeability and low redox potential. *J Nucl Med* 38: 1155–1160, 1997.
9. Fujibayashi Y, Taniuchi H, Wada A, Yonekura Y, Konishi J, Yokoyama A. Differential mechanism of retention of Cu-pyruvaldehyde-bis(N^4-methylthiosemicarbazone) (Cu-PTSM) by brain and tumor: a novel radiopharmaceutical for positron emission tomography imaging. *Ann Nucl Med* 9: 1–5, 1995.
10. Wada K, Fujibayashi Y, Tajima N, Yokoyama A. Cu-ATSM, an intracellular-accessible superoxide dismutase (SOD)-like copper complex: evaluation in an ischemia-reperfusion injury model. *Biol Pharm Bull* 17: 701–704, 1994.
11. Lewis JS, McCarthy DW, McCarthy TJ, Fujibayashi Y, Welch MJ. Evaluation of ^{64}Cu-ATSM *in vitro* and *in vivo* in a hypoxic tumor model. *J Nucl Med* 40: 177–183, 1999.
12. Matsumoto K, Fujibayashi Y, Yonekura Y. Application of the new zinc-62/copper-62 generator: an effective labeling method for ^{62}Cu-PTSM. *Nucl Med Biol* 19: 39–44, 1992.
13. Gingas BA, Suprunchuk T, Bayley CH. The preparation of some thiosemicarbazones and their copper complexes. Part III. *Can J Chem* 40: 1053–1059, 1962.
14. DeGrado TR, Turkington TG, Williams JJ, Stearns CW, Hoffman JM, Coleman RE. Performance characteristics of a whole-body PET scanner. *J Nucl Med* 35: 1398–1406, 1994.
15. Herscovitch P, Markham J, Raichle ME. Brain blood flow

measured with intravenous $H_2{}^{15}O$. I. theory and error analysis. *J Nucl Med* 24: 782–789, 1983.
16. Raichle ME, Martin WRW, Herscovitch P, Mintun MA, Markham J. Brain blood flow measured with intravenous $H_2{}^{15}O$. II. implementation and validation. *J Nucl Med* 24: 790–798, 1983.
17. Meyer E. Simultaneous correction for tracer arrival delay and dispersion in CBF measurements by the $H_2{}^{15}O$ autoradiographic method and dynamic PET. *J Nucl Med* 30: 1069–1078, 1989.
18. Fujibayashi Y, Yoshimi E, Waki A, Takahashi N, Yonekura Y. Cu-ATSM, a new tumor agent predicting ability for bioreductive drug activation. *J Nucl Med* 39 (suppl): 90P, 1998. [abstract]